



Studies on doping concentration effect of CdS quantum dots in active layer of hybrid bulk heterojunction (P3HT:PCBM) polymer solar cells

S.V. Borse

Associate Professor, Dept. of Physics, S.S.V.P.S's ASC College, Shindkheda (M.S.), India-425406

Email - sv5517@gmail.com

Abstract: In this article, the process of making the hybrid bulk heterojunction (BHJ) polymer solar cells and their performance is discussed. The solar cells are made by mixing CdS nanoparticles (QDs) into a blend of a conjugated polymer called P3HT (poly(3-hexylthiophene)) and a fullerene-based material known as PCBM (phenylC61-butyric acid methyl ester), which is used as the acceptor. Dichlorobenzene and chlorobenzene are used as solvents. CdS nanoparticles in different amounts were added to a fixed amount of the P3HT and PCBM blend. The samples were tested using various methods like X-ray diffraction (XRD), atomic force microscopy (AFM), scanning electron microscopy (SEM), transmission electron microscopy (TEM), ultraviolet-visible (UV-VIS) spectroscopy, and I-V and power conversion efficiency (PCE) measurements. Adding CdS nanoparticles improves the structure of the active layer, making it more uniform, which leads to better light absorption and electrical conductivity. XRD results show that the way P3HT crystallizes is affected by how much CdS is mixed into the blend. When CdS QDs are mixed into the polymer blend, it increases the efficiency of the solar cells under normal light. The efficiency went from 1.3% to 4.0%, mainly due to higher fill factor (FF) and short-circuit current (J_{sc}) when the right amount of CdS nanoparticles was added. The increase in J_{sc} happened because the CdS nanoparticles formed a network inside the P3HT: PCBM blend. The presence of CdS nanoparticles also improved light absorption in the visible range because of their high absorption rate and long charge transport properties. The overall performance of the solar cells improved because of better J_{sc} , V_{oc} , FF, and PCE, which is due to reduced charge recombination in the CdS-doped devices.

Key Words: Solar cell, Bulk heterojunction, CdS NPs, P3HT: PCBM.

1. INTRODUCTION: Solar cells made from organic polymer materials have several good features. They can be made using low-cost methods, have high production rates, and absorb light very well. These materials can be deposited on flexible surfaces because they work at low temperatures. Quantum dots are a type of semiconductor. Their electronic behavior depends on their size and shape. Smaller dots have a larger band gap, which means more energy is needed to excite them, and more energy is released when they return to their normal state. The quantum confinement effect shows that when the size of a quantum dot is smaller than 100 nm, the energy gap becomes wider. This causes a blue shift in the energy levels of the excitons (26). Quantum dot solar cells are a new type of solar cell that uses multiple layers of photovoltaic materials (6). By changing the size of the quantum dots, their energy gap can be adjusted. Many researchers have studied using cadmium sulfide nanoparticles (CdS NPs) as a sensitizer in solar cells (7–9). However, organic solar cells face some challenges. They are sensitive to heat, moisture, oxygen, and UV light (10). Bulk heterojunction polymer solar cells are promising for flexible and large-area panels because they can be made using low-cost techniques (11–12). These cells use a combination of a polymer called P3HT as an electron donor and another material called PCBM as an electron acceptor (13,14). Liquid-phase polymer solar cells perform worse compared to inorganic solar cells like silicon or CIGS-based ones. This is due to low charge movement and short diffusion lengths in the active layers. To improve performance, the layer thickness and annealing temperature can be optimized. Choosing the right donor and acceptor materials helps, as does using a buffer layer (16,17). Another issue with organic materials is their low dielectric constant, which causes excitons (bound electron-hole pairs) to form instead of free charges. Differences in the internal fields between the donor and acceptor help break these excitons. To solve this, inorganic semiconductor nanostructures are added to create hybrid devices. These combinations offer better charge movement, charge drift, and stability compared to pure organic materials. Researchers like Sankara Rao Gollu et. al. (18) have used copper sulfide (CuS) nanoparticles in P3HT:PCBM to increase the open circuit voltage, shortcircuit current, fill factor, and power conversion



efficiency by over 100%. V.D. Mihailetschi et. al. (19) found that mixing lead sulfide (PbS) nanoparticles in a blend increased efficiency by 30%. Using titanium dioxide (TiO₂), nickel oxide (NiO), and copper oxide (CuO) nanoparticles instead of P3HT and PCBM also improved efficiency. The best results were seen with the right concentration of these nanoparticles (20). Other materials like PbSe, CdSe, PbS, FeS₂, In₂S₃, and CdS have also been used with polymers to boost performance (21–25). Small nanoparticles increase the surface area between the donor and acceptor, helping charges separate in the active layer. Quantum dots are good for hybrid solar cells because they offer better electron mobility, stability, and light absorption (26). To make better hybrid quantum dot solar cells, we need to control how light interacts with both organic and inorganic materials. Increasing the interface area and phase separation will help. CdS nanoparticles are useful in solar cells and act as an electron transfer layer. They have also been used in bulk heterojunction cells to improve absorption and efficiency (27). In this study, CdS quantum dots were made at different concentrations (1, 2, and 4 wt%) and added to the active layer of P3HT:PCBM. These layers were placed between an ITO electrode coated with PEDOT:PSS and an aluminum anode. The films were tested using various methods to find out their surface shape, thickness, roughness, optical, and electrical characteristics.

2. Experimental section:

2.1 MATERIALS: ITO-coated glass was bought from Intelligent Materials Pvt. Ltd. and had a sheet resistance between 10 and 15 ohms per square. The hole injector layer (HIL) used PEDOT: PSS, a type of conductive polymer, and also included P3HT, a highly ordered polymer, and PCBM, a type of organic semiconductor. These materials were obtained from Sigma-Aldrich. Cadmium nitrate (Cd(NO₃)₂·4H₂O), ethanol (C₂H₆O), and thiourea (NH₂-CSNH₂) were purchased from BDH as high-quality analytical grade chemicals.

2.2 PREPARATION OF CdS NANOPARTICLES: To make CdS quantum dots, a chemical bath deposition (CBD) method was used. First, 0.1 M of cadmium nitrate was dissolved in 20 ml of ethanol at room temperature. Then, 0.1 M of thiourea was added to the same solution, along with oleic acid to keep the nanoparticles from growing too large. The ITO glass was dipped into the solution for 10 minutes. After that, the CdS film was dried in a hot air oven for a few minutes. At the bottom of the beaker, CdS nanoparticles formed along with some solvent byproducts. These were separated using a centrifuge for 15 minutes. The purified CdS nanoparticles were then washed several times with 2-propanol or hexane and finally kept in hexane for storage.

2.3 DEVICE FABRICATION: The device was built as shown in Figure 1. The ITO glass was cleaned in an ultrasonic bath for 10 minutes using soap, ethanol, and acetone and then rinsed with distilled water and dried under nitrogen gas. A thin layer of PEDOT: PSS, about 50 nm thick, was applied using spin coating at 2500 rpm for 80 seconds. The PEDOT: PSS layer was heated on a hot plate at 120°C for 20 minutes to make the surface smoother. Next, a mixture of P3HT, PCBM, and CdS nanoparticles in different weight ratios (1:0.8:0, 1:0.8:0.1, 1:0.8:0.2, and 1:0.8:0.4) was dissolved in a mixture of chlorobenzene and dichlorobenzene (2:1). These solutions were stirred overnight at 45°C before being applied onto the PEDOT: PSS layer through spin coating. The resulting films were then heated at 110°C for 10 minutes in a nitrogen-filled glove box. Finally, a LiF layer (10 nm) and aluminum contacts (100 nm) were deposited using a high vacuum deposition system over the heated films. The active area of the device was kept at 30 mm² using a shadow mask.

2.4 CHARACTERIZATION:

The structure and size of the CdS nanoparticles were studied using a grazing incidence X-ray diffractometer (Siemens D5000) with Cu-K α radiation (wavelength of 1.5406 Å). The measurements were taken from 10 to 80 degrees in 0.05-degree steps, with a count time of 5 seconds per step. The surface morphology and size of the deposited films were examined using a high-resolution scanning electron microscope (JEOL 2010F) and an atomic force microscope (Digital Instruments Nanoscope IV). HRTEM analysis was performed on a JEOL JEM-2010 FEG instrument with a point resolution of 1.9 Å. The absorption spectra were collected using a Systronics 110 UV-VIS spectrophotometer with a PC interface. The current-voltage (J-V) curves were measured in a nitrogen-filled glove box using a solar simulator and a Keithley 2420 source meter under standard conditions (AM 1.5 G, 100 mW/cm² irradiation).

3. RESULT AND DISCUSSION:

3.1 STRUCTURAL STUDIES:

Fig. 2 shows the powder X-ray diffraction (XRD) patterns of the as prepared CdS QDs by above given method. The observed peaks of the as-prepared CdS NPs show a hexagonal close-packed (hcp) structure and match with the JCPDS card 02-0454. The estimated crystallite size of CdS nps is around 18.60 nm and it is calculated from the Debye Scherrer's formula (29). Three main diffraction peaks are seen at $2\theta = 26.6^\circ$, 43.98° and 52.23° which are related to the (111), (220) and (311) reflections of cubic CdS. The X-ray diffraction profiles clearly shown that the intensity of the (111) peak is higher than other crystalline phases. The deposited CdS NPs grow with Face Centered Cubic (FCC)

structure. The diffraction patterns of the films are found to be matched with the JCPDS card 10-0454. The maximum intensity diffraction peak appearing at $2\theta = 26.6^\circ$ and it is of the (111) plane of the cubic CdS (30, 31). The calculated value of the lattice constant is closely matched with standard value (5.818 Å - JCPDS Card. 10-0454). The slight increases of the lattice constant for the reported values were observed (32). The average value of the crystallite size (D) can be obtained from the Debye-Scherrer's Equation. The crystallite size is found to be 1.92, 2.72 and 3.15 nm for (111), (200) and (311) reflection plane, respectively.

3.2 SURFACE MORPHOLOGICAL STUDIES:

Figure 3 shows the FESEM images of the P3HT: PCBM and CdS NPs incorporated in P3HT: PCBM blend. The image shows that the film material is completely spread over the substrate surface in the form of nano sized particles with an average grain size of 20 nm. From the FESEM images it could be observed that the surface of the substrate is completely covered with the QDs. The surface morphology of the crystalline film is coarse and the granules in the films are uniformly distributed. From above images it is observed that as the CdS wt % increases, there is increase in coarseness of CdS NPs on films surface. The Atomic Force Microscopy (AFM) measurements were performed to evaluate the topographical characteristics of the CdS NPs on thin layers. Fig.4. shows the 2D and 3D AFM images of the CdS NPs with a scanning area of 100 x 100 nm respectively.

Fig. 1. Schematic diagrams of (a) glass ITO/HIL/P3HT: PCBM: CdS NPs/LiF / Al bulk heterojunction solar cell device.

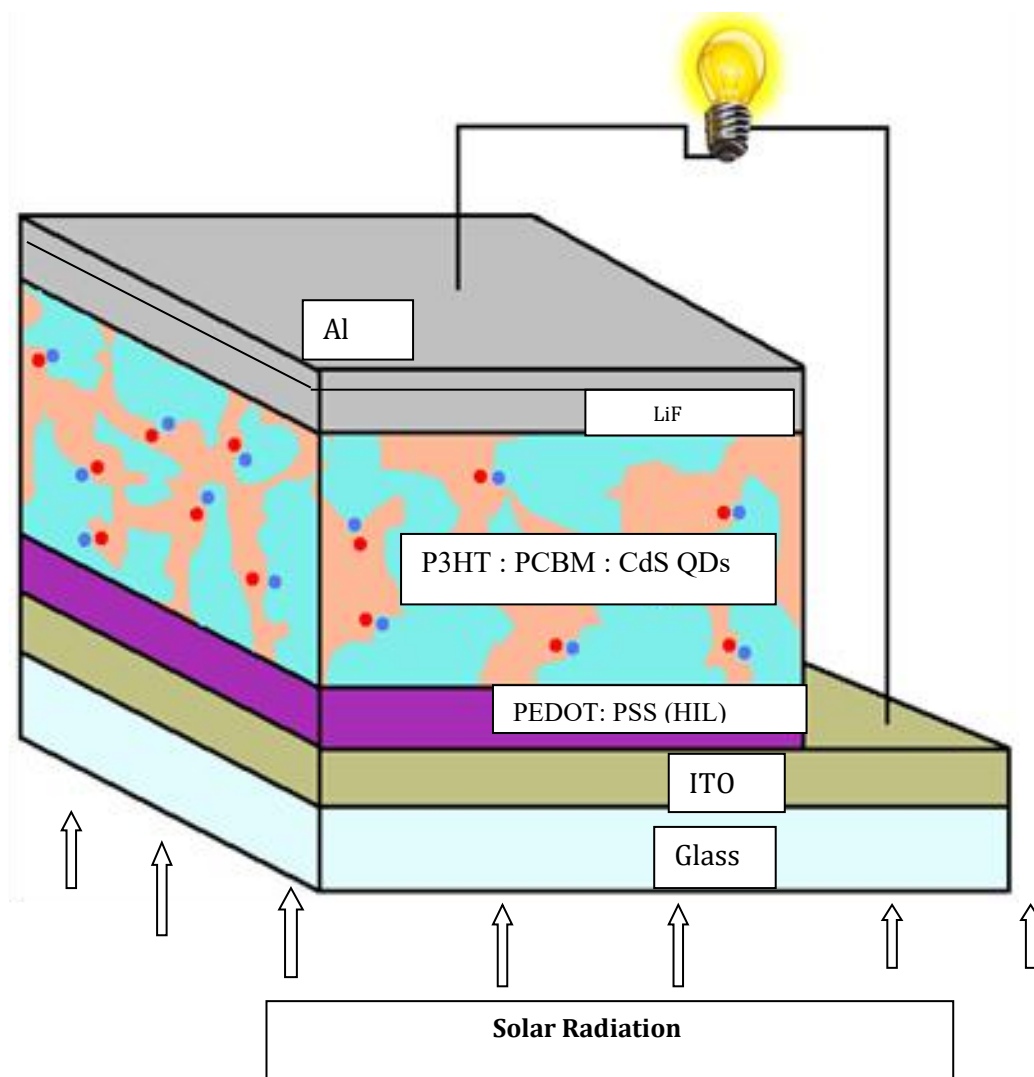


Fig. 2 Powder X-ray diffraction (XRD) patterns of the as prepared CdS QDs.

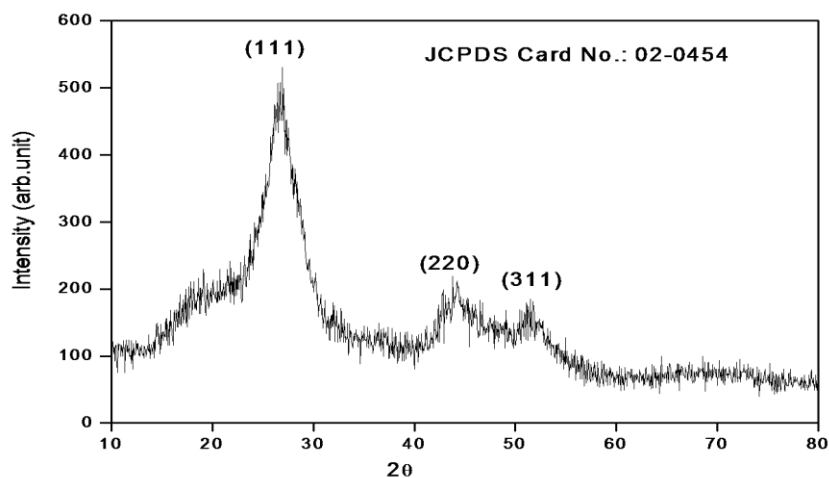
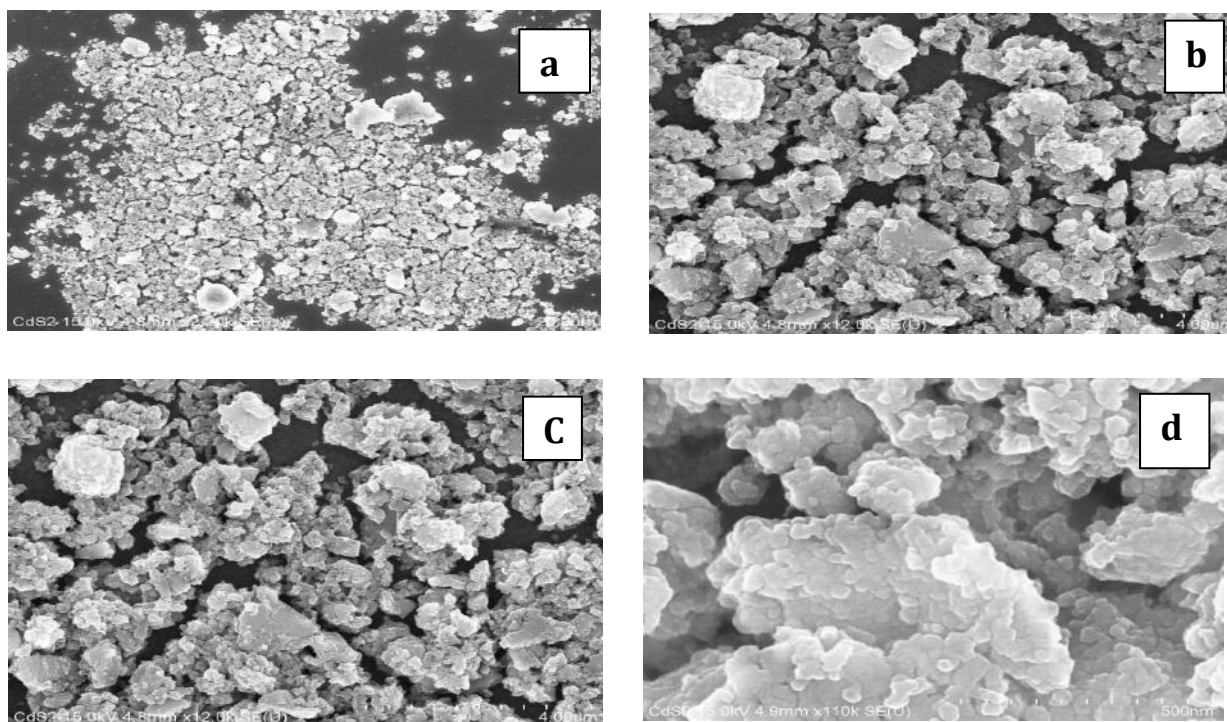


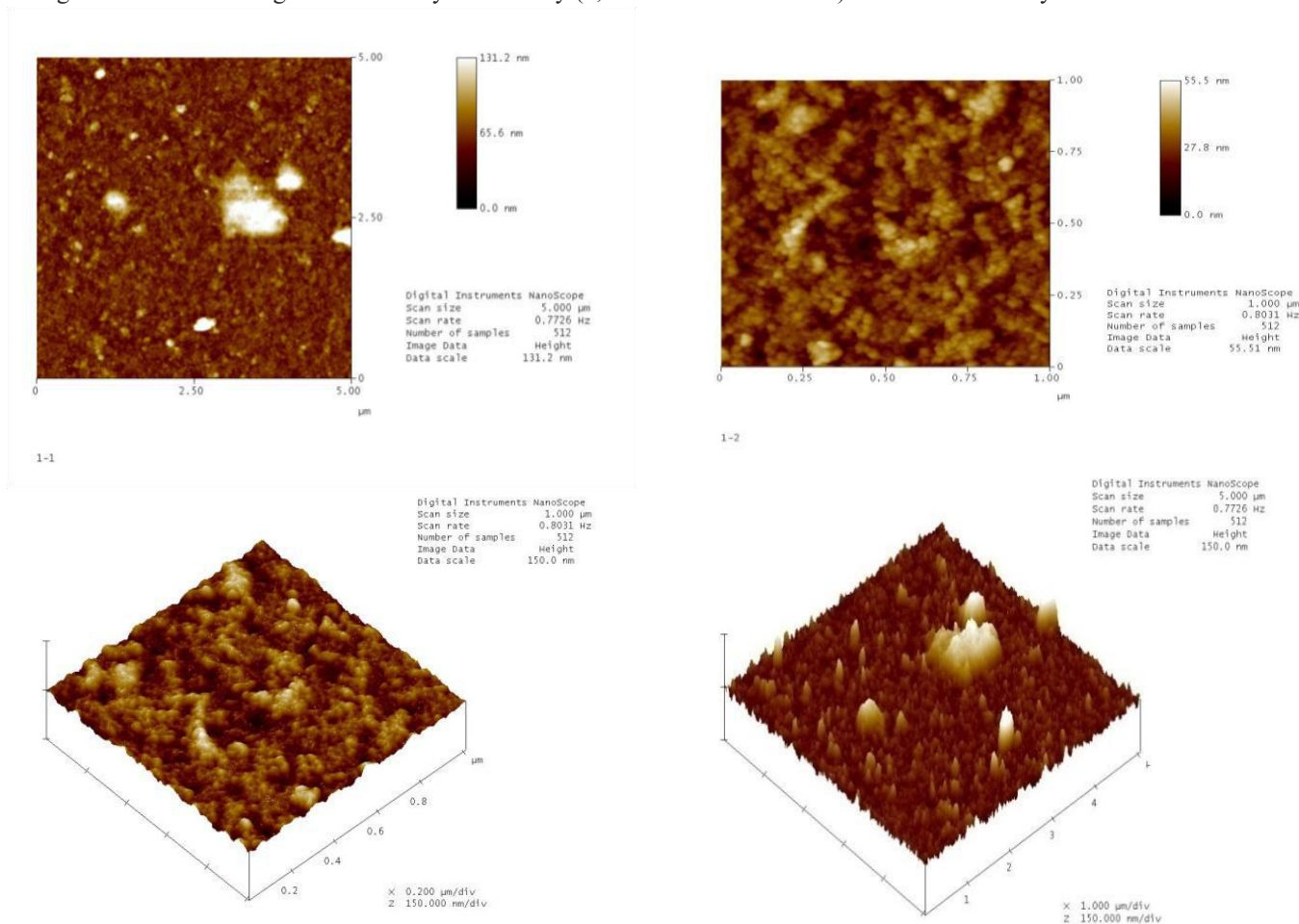
Fig. 3 FESM micrograph of binary and ternary blend materials surface. a) 0 wt % b) 1 wt % c) 2 wt % and d) 4 wt %



The particles are all the same size and spread out in all directions. The average surface roughness (R_a) ranges from 17.20 to 23.25 nm, the height ranges from 55.5 to 131.2 nm, and the particle sizes are between 31 nm and 38 nm. The CdS NPs are randomly spread on top of the polymer film and their surfaces are smooth. Some of the CdS NPs form large, grouped sphere shapes. The 3D-AFM images in Fig. 4d show that the grains are spread out evenly over a 100 nm x 100 nm area, with some grains sticking up. This surface property is important for solar cells [33,34].

The image also shows that the film is continuous with well-connected grains and no holes, cracks, or big clumps. Fig. 5(a) shows a TEM image of CdS NPs made at 230°C for 12 hours. Fig. 2(a) is a TEM image of CdS NPs, showing they are spherical and their size is about 38 nm. Fig. 2(b) shows the interplanar lattice spacing for the (112) plane, calculated from the HR-TEM image, which is 3.2 Å.

Fig. 4 shows AFM images of the binary and ternary (1, 2 and 4 wt% CdS NPs) blended active layers in 2D and 3D formats



3.3 CELL PERFORMANCE PARAMETERS:

To find the best performing device, J– V characteristics of different concentrations were tested under light intensity of 100 mW cm^{-2} (Fig. 6). The plot shows that PCE increases as more CdS NPs are added to the active layer of the P3HT: PCBM blend. The PCE goes from 1.3% to 4.0% at the best CdS NPs concentration. This improvement is because adding NPs increases the fill factor (FF) and the short circuit current (J_{sc}). Four different amounts of NPs were mixed into the active layer blends. Their electrical parameters are shown in Fig.6 listed in Table 1. The network formed by CdS NPs in the active layer helps improve PCE. Mixing NPs increases J_{sc} by helping with more light absorption and forming a better connected network of CdS NPs in the P3HT:PCBM blend. CdS NPs also allow faster charge transfer at the interface and minimize electron-hole recombination losses (35). Adding CdS NPs to the active layer changes the energy levels between P3HT and the conduction band of CdS. This can help in improve the open-circuit voltage (V_{oc}) of the device (36,37). In this case, adding small amounts of CdS NPs keeps the V_{oc} steady. The poor performance of the cell with a ratio of 1 : 0.8 : 0.4 is because CdS NPs bunch together. Too many NPs in the blend can break up the network for better charge movement.

Fig.5. (a) TEM image of CdS NPs, (b) HRTEM image of CdS NPs.

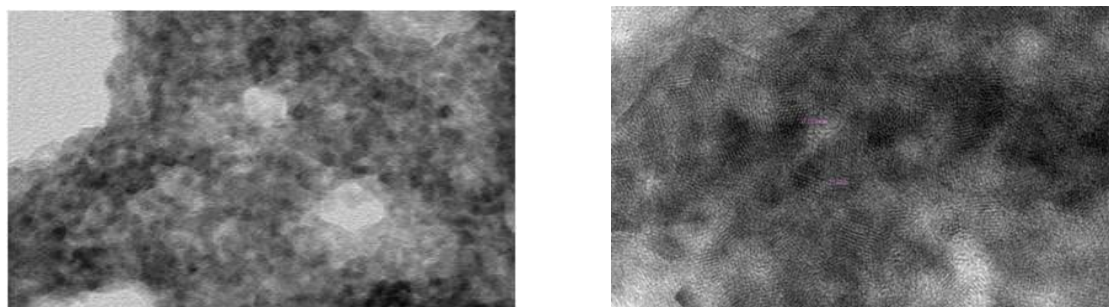


Fig. 6.J–V curves of binary and ternary blended hybrid organic solar cells

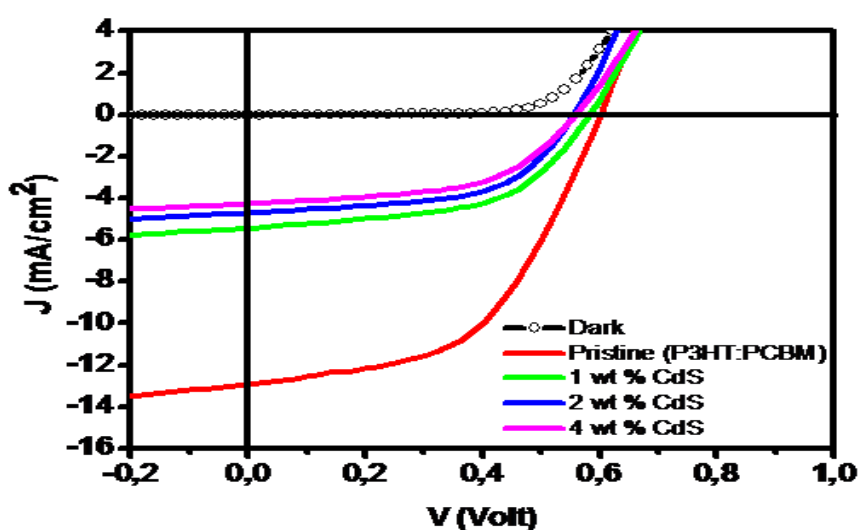
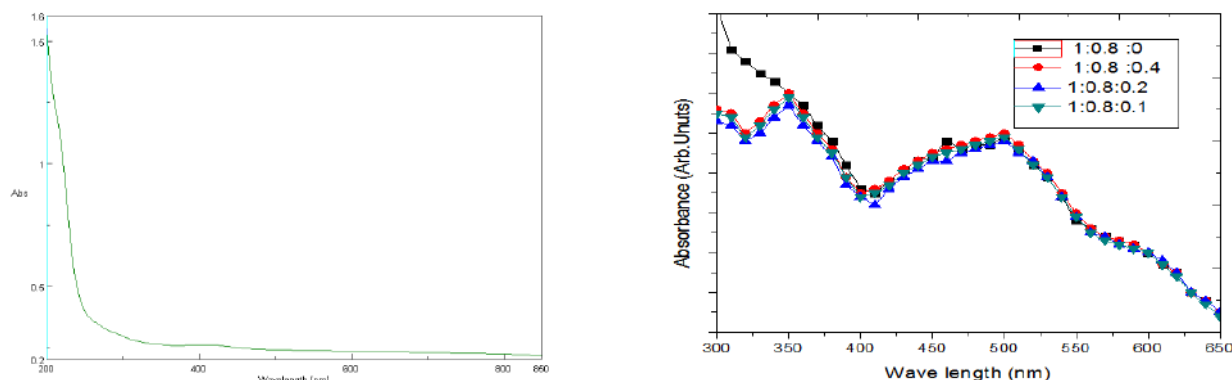


Table: 1 Device parameters obtained from the J–V curves shown in Fig. 5.

| CdS (wt %) | P3HT : PCBM : CdS (wt %) | Jsc (mA cm ⁻²) | Voc (V) | FF (%) | PCE (%) |
|------------|--------------------------|----------------------------|---------|--------|---------|
| 0 | 1 : 0.8 : 0 | 12.9 | 0.6 | 51.7 | 1.4 |
| 1 | 1 : 0.8 : 0.1 | 5.44 | 0.58 | 53.9 | 2.6 |
| 2 | 1 : 0.8 : 0.2 | 4.71 | 0.55 | 56.4 | 4 |
| 4 | 1 : 0.8 : 0.4 | 4.26 | 0.55 | 54.3 | 1.3 |

To check how well the NPs spread in the P3HT:PCBM blend, FESEM images of the film were taken. The SEM images of P3HT:PCBM and CdS-NPs mixed (1, 2, and 4 wt%) blends are shown in Fig. 3(a–d). Fig. 3a shows a smooth surface for CdS NPs at 0 wt% (1 : 0.8 : 0), which is easier to make than blends with CdS NPs. The optimized CdS NPs (1, 2, 4 wt%) form a connected network of P3HT:PCBM:CdS on the surface, which is good for electron movement in the active layer. However, when too much CdS-NPs is used (1 : 0.8 : 0.4), the film becomes crowded with NPs, as seen in Fig. 3d. AFM images show the surface texture, roughness, and clumping of CdS NPs in the P3HT:PCBM blend, as shown in Fig. 4. The undoped material P3HT:PCBM (Fig. 4a) has a smooth surface with an RMS value of 2.24 nm. Adding 1% CdS NPs (Fig. 4b) makes the surface rougher, with an RMS of 3.25 nm. Further addition of CdS NPs increases the RMS to 4.20 nm (Fig. 4c) and 4.55 nm (Fig. 4d) for 2% and 4% CdS NPs, respectively. The UV-VIS absorption spectra for CdS NPs and the doped P3HT:PCBM:CdS NPs blend are shown in Fig. 7(a and b). The absorption increases with more NPs in the visible range in the P3HT and PCBM structure.

Fig. 7. (a) UV–VIS–NIR absorption spectroscopy of CdS nanoparticles (b) Absorption spectra of P3HT:PCBM : CdS NPs blended thin films in the visible region.



In the absorption spectra, CdS NPs in the P3HT:PCBM blend are visible near 335 nm compared to the pure film (1 :0.8: 0). The better light absorption in the visible range is due to increased film roughness, which helps with light scattering and improves the efficiency of converting light photons into current (38).

4. CONCLUSION:

The hybrid organic binary heterojunction solar cells were successfully developed by blending various ratios of CdS NPs in the active layer of P3HT: PCBM blend. The optimum wt% proportion of CdS, NPs in the P3HT: PCBM blend and use of proper HIL material shows higher photo conversion efficiency as compared with the 0 wt% of CdS NPs added device. In present work PCE is improved from 1.3 to 4.0 %. The important reason for betterment in PCE was due to the improvement in Jsc and FF with CdS- NPs addition and conjugated active layer of the devices. Solar cell related all electrical parameters and PCE of the doped devices increased with the increasing incorporation of CdS NPs in the active layer of P3HT:PCBM blend. The hole injector layer (HIL) material is PEDOT: PSS – poly (3, 4-polyethylene dioxythiophene polystyrene sulfonate) also plays a main role in improvement of PCE. The photo absorption in the doped active layers increased in the visible region as compared to the non CdS doped polymer active layer. The film roughness increased with doping, and higher ratio of NPs in the active layer showed clustering and damaged in long penetrating network, gives to reduced performance of the devices; this suggested that PCBM has an important role as a surfactant material for the CdS - paired active layer.

ACKNOWLEDGMENT:

Author S.V.Borse is thankful to Dr. Sudam Chavhan for characterization of samples and cooperation in fabrication of the device and calculations of performance parameters of device.

REFERENCES:

1. X. Dong, P. Shi, L. Sun, J. Li, F. Qin, S. Xiong, T. Liu, X. Jiang, Y. Zhou, (2019) : *J. Mater. Chem.* 7 1989–1995.
2. R. Yu, H. Yao, L. Hong, Y. Qin, J. Zhu, Y. Cui, S. Li, J. Hou, (2018): *Nature Communications* volume 9, Article number: 4645 (2018) 9 1–9.
3. Halperin, W. P. (1986): *Mod. Phys.*, Vol. 58, No. 3, , pp. 533-607.
4. Lippens, P. E. and Lannoo, M., (1989) : *Phys. Rev. B*, Vol. 39, No. 15, pp. 10935- 10942.
5. Khairutdinov, R. F., (1998): *Russ. Chem. Rev.*, Vol. 67, No. 2, pp. 109-122.
6. B. O'Regan, M. Grätzel, (1991): *Nature* 353, 737
7. Sheng-chih Lin, Yuh-Lang Lee, Chi-Hsiu Chang, Yu-Jen Shen, and Yu-Min Yang (2007): *Applied Physics Letters* 90, 143517
8. S. Wageh, A.A. AL-Ghamdi, M. Soylu, Y. AL-Turki and F. Phanogolu (2013) : *ACTA PHYSICA POLONICA*, Vol. 124
9. R. Chalita, C.R. Xiong, Jr, J.B. Kenneth (2008): *ACS Nano* 2, 682.
10. R. Sorrentino, E. Kozma, S. Luzzati, R. (2021) : *Energy Environ. Sci.* 14 180–223.
11. Khairutdinov, R. F (1998): *Russ. Chem. Rev.*, Vol. 67, No. 2, , pp. 109-122.
12. Lippens P.E., and Lannoo (1989): *Phys. Rev. B* vol. 39 No. 15 pp 10935-10942



13. Rajeshwar, K., and Chenthamarakshan, C. R., (2001) : *Chem. Mater.*, Vol. 13, , pp. 2765-2782
14. Sheng-chih Lin, Yuh-Lang Lee, Chi-Hsiu Chang, Yu-Jen Shen, and Yu-Min Yang(2007): *Applied Physics Letters* **90**,143517
15. S. Wageh,A.A. AL-Ghamdi,M. Soylu,Y. AL-Turki and F. Phanogolu(2013) : *ACTA PHYSICA POLONICA*, Vol. 124 .
16. R. Chalita, C.R. Xiong, Jr, J.B. Kenneth: *ACS Nano* 2, 682
17. Halperin, W. P(1986): *Mod. Phys.*, Vol. 58, No. 3, , pp. 533-607.
18. Sankara rao gollu,R.sharma G.Shrinivas Souvik Kandu(2014): *Organic electronics: 15 (10) pp*2518-2525.
19. V.D. Maihailcith, H. X. Xie, B.de Boer, L.J.A Koster.(2006):*Advanced functional materials*Vol.16 issue- 5 pp 699-708.
20. M. Imran, M. Ikram, A. Shahzadi, S. Dilpazir, H. Khan, I. Shahzadi, S.A. Yousaf, S. Ali, J. Geng, Y. Huang, (2018) :*RSC Adv.* 8 18051–18058.
21. S.j.Kim,W.J.Kim,AN Cartwrite, PN Prasad.(2008) : *Appl. Phys.Lett*Vol. 92,Issue 19.
22. Ligli Luo, Weling Luan, Binxia Yaun, Chengaxi Zhang, Lin Jin (2015): *Energy Proceedia*. Vol.75 pp 2181-2186.
23. Ferhat Aslan, Gatachew adam, Philip Stadler, Niyazi Serdev(2014) : *Solar Energy* Vol.108 pp 230-237
24. M.Junkeer Khan, Ranoo Bhargav, Amarjeet Kaur, S.K.Dhavan(2010),:*Solar Energy* vol.519 issue 3 pp 1007-1011.
25. Neelesh kumar, Viresh Dutta, : (2014) *J.Colloid and interface Sci.* Vol.434. pp 181-187.
26. Acevedo, A. M., (2006) : *Sol. Energy Mater. & Sol. Cells*, Vol. 90, No. 15, , pp. 2213-2220
27. N. Zhou, G.P. Chen, X.L. Zhang, L.Y. Cheng,Y.H. Luo, D.M. Li, Q.B. Meng(2012): *Electrochem. Comm.*20, 97.
28. K. veerthangam, Mutha Senthil Pandiyan,P.Rama swami(2014): *Int. Jourl. of chem. Tech. research* Vol.6 No.13 pp 5396-5399.
29. Senthamilselvi, V., K. Ravichandran and K. Saravanakumar,(2013): *J. Phys. Chem. Solids*, 74: 65-69. DOI: 10.1016/j.jpcs.2012.07.020
30. Oladeji, I.O., L. Chow, J.R. Liu, W.K. Chu and A.N.P. Bustamante *et al.*,(2000) : *Thin Solid Films*, 359: 154-159. DOI: 10.1016/S0040-6090(99)00747-6
31. Cortes, A., H. Gomez, R.E. Marotti, G. Riveros and E.A. Dalchiale, 2004. : *Solar Energy Mater. Solar Cell*, 82: 21-34. DOI: 10.1016/j.solmat.2004.01.002.
32. Martinez, M.A., C. Guillen and J. Herrero, (1988):*Applied Surf. Sci.*, 136: 8-16. DOI: 10.1016/S0169-4332(98)00331-6
33. N. N. Jandow, M. S. Othman, N. F.Habubi, S. S. Chiad, K. A. Mishjil, I. A. Al-Baidhany, (2020):*Materials Research Express*, 6 (11),
34. M. D. Sakhil, Z. M. Shaban, K. S. Sharba, N. F. Habub, K. H. Abass, S. S. Chiad, A. S. Alkelaby, (2020) *NeuroQuantology*, 18 (5), 56-61
35. L.D.Wang, D.X. Zhao, Z.S. Su, D.Z. Shen, (2012).:*Nanoscale Res. Lett.* 7, 106
36. Z. Li, X. Li, Y. Zong, G. Tan, Y. Sun, M. He, Z. Ren, X. Zheng, (2017): *Carbon* 115 493–502
37. X. Dong, P. Shi, L. Sun, J. Li, F. Y. Zhou(2019): *J. Mater. Chem.* 7 1989–1995.
38. M. Ikram, R. Murray, A. Hussain, and S. Ismat Shah(2014): *Mater. Sci. Eng., B*, 189, 64–69.